

25 electrical COP_{el} of 2.62 are achieved respectively under steady operating condition at
26 CaCl₂ concentration ratio of 36%.

27

28 *Keywords:* Liquid desiccant, Dehumidification, Regeneration, Membrane,
29 Experimental tests

30 * Corresponding author: Tel: +44 1158466141

31 E-mail address: jie.zhu@nottingham.ac.uk.

32 **Nomenclature**

c_p	Specific heat capacity (J/kg.K)
h	Specific enthalpy (J/kg.K)
m	Mass (kg)
\dot{m}	Mass flow rate (kg/s)
\dot{M}	Moisture change rate (g/s)
P	Pressure (Pa)
\dot{Q}	Input/ Output Power (W)
T	Temperature (°C)
x_i	Measured variable
U_x	Measured variable uncertainty
U_y	Variable uncertainty
v	Volumetric flow rate (L/min)
V	Volume (m ³)
W_e	Total electrical requirement (W)

Greek symbols

η	Effectiveness
ρ	Density (kg/m ³)
ω	Air humidity ratio (kg/kg _{dryair})

Subscripts

a	Moisture addition
air	Air
c	Cooling
eq	Equilibrium state
fl	Flow meter float
in	Inlet
out	Outlet
r	Moisture removal
sol	Solution
w	Water

Abbreviations

COP	Coefficient of performance
DH	Dehumidifier
RE	Regenerator

33

34

35

36

37

38

39

40 **1. Introduction**

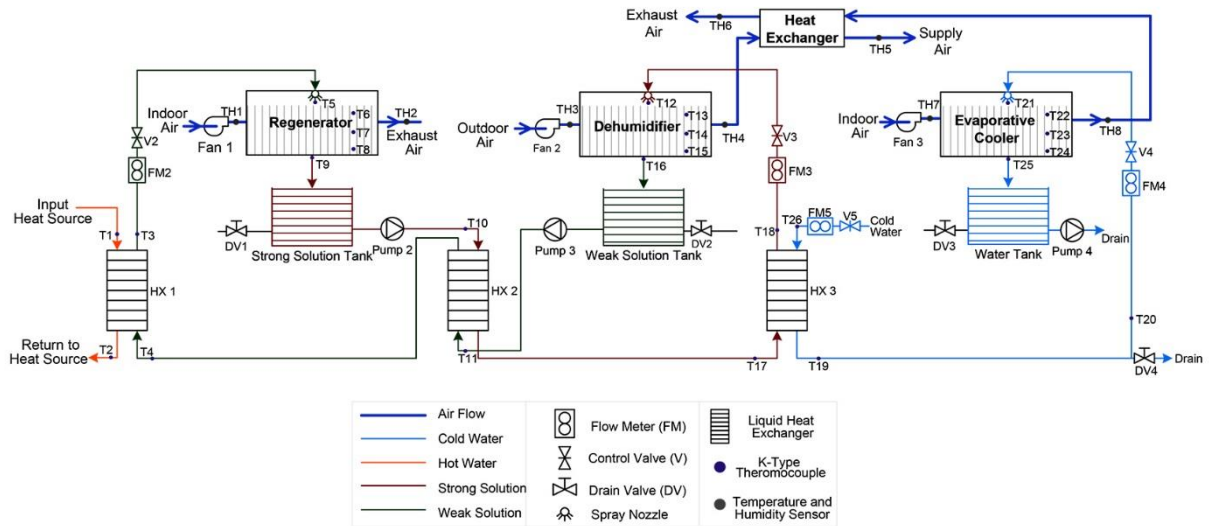
41 Desiccant cooling has been regarded as an environmental-friendly air conditioning
42 technology without shortcomings of overcooling and reheating [1]. Compared to the
43 solid desiccant system, the liquid desiccant system is more economical and flexible in
44 utilization of low-grade energy sources [2] and efficient in providing high quality
45 supply air with independent humidity and temperature controls [3]. Generally, the
46 selection of a liquid desiccant depends on various parameters, like boiling point
47 elevation, energy storage density, regeneration temperature, thermophysical property,
48 availability and cost [4]. Particularly, halide salts are mostly preferred, for example
49 lithium chloride (LiCl), lithium bromide (LiBr) and calcium chloride (CaCl₂).
50 Comparatively, CaCl₂ is the cheapest and most readily available desiccant [5]. On the
51 other hand, a variety of packing types of the liquid desiccant system have been
52 developed, such as wetted wall, spray tower, packed column and membrane-based [6].
53 Among them, the membrane-based configuration providing an indirect contact for
54 dehumidification has attracted more interests owing to the elimination of solution
55 carryover problem. In operation, membranes allow heat and moisture transfer between
56 solution and process airstream, whereas meanwhile prevent the entrainment of liquid
57 desiccant [7].

58 Many studies of the membrane-based liquid desiccant cooling system have been
59 conducted, which incorporates different renewable energy sources and cooling
60 technologies. For instance, Abdel-Salam, et al. [8] proved the feasibility of a
61 membrane-based desiccant air conditioning system powered by solar energy. El-
62 Dessouky, et al. [9] proposed a new air conditioning system consisting of a membrane
63 dehumidification unit and a direct evaporative cooler, and they observed that 86.2%
64 energy saving can be achieved compared to a conventional stand-alone vapour

65 compression system. In addition, Jradi and Riffat [10] developed a hybrid
66 dehumidification cooling system integrated with an indirect evaporative cooler, with
67 which the supply air temperature and humidity reduce from 33.8°C to 22.3°C and 68.6%
68 to 35.5% respectively. However, yet limited researches have been carried out for
69 feasibility study and performance evaluation of the membrane-based liquid desiccant
70 dehumidification cooling system through experimental work. In this study, a
71 membrane-based hybrid dehumidification cooling system with heat recovery is built
72 for experimental investigations. Feasibility of the system for hot and humid regions is
73 assessed and influences of various operating variables, including inlet air condition,
74 desiccant concentration ratio and regeneration temperature on the dehumidifier,
75 regenerator and overall system performances are evaluated based on the experimental
76 results.

77 **2. Experimental set-up**

78 The proposed hybrid system is mainly composed of a dehumidifier, a regenerator, an
79 evaporative cooler and an air-to-air heat exchanger, as shown in Fig. 1. Three processes
80 are involved during operation, namely: dehumidification, regeneration and evaporative
81 cooling. Additionally, the airstream from the evaporative cooler is used to cool the dry
82 air to meet the supply requirement in the air-to-air heat exchanger. After
83 dehumidification, the dilute solution flows into the weak solution storage tank and is
84 delivered by magnetic-driven pump to a heat exchanger (HX2), where the weak
85 solution is pre-heated before being heated by heat source. To enhance the
86 dehumidification performance, cold water cools the strong desiccant solution prior to
87 flowing into the dehumidifier and then flows directly into the evaporative cooler.



88

89

Fig. 1. Schematic graph of the membrane-based dehumidification cooling system

90

Membrane-based units for the dehumidifier and regenerator are designed with a

91

dimension of 410mm (Length) × 230mm (Width) × 210mm (Height), as depicted in

92

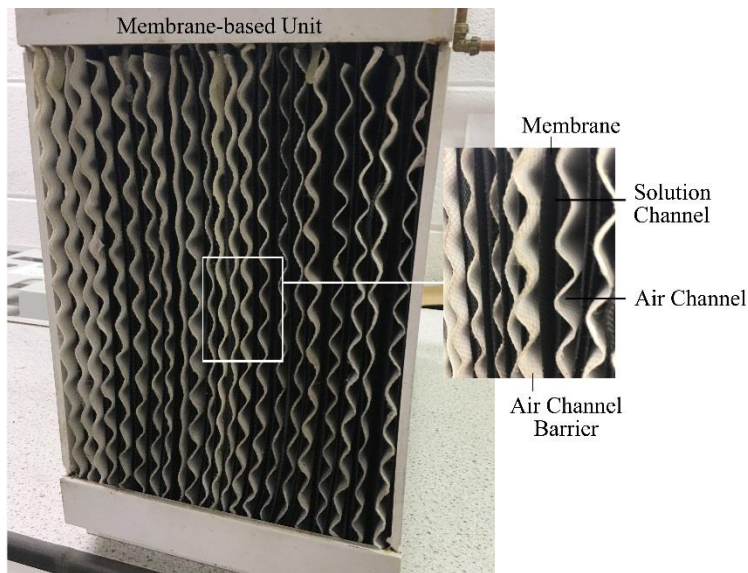
Fig. 2. For the evaporative cooler with the same dimension, air channels are formed by

93

fibre without membrane sheets, which provides wet surface as cold water flowing

94

downwards.



95

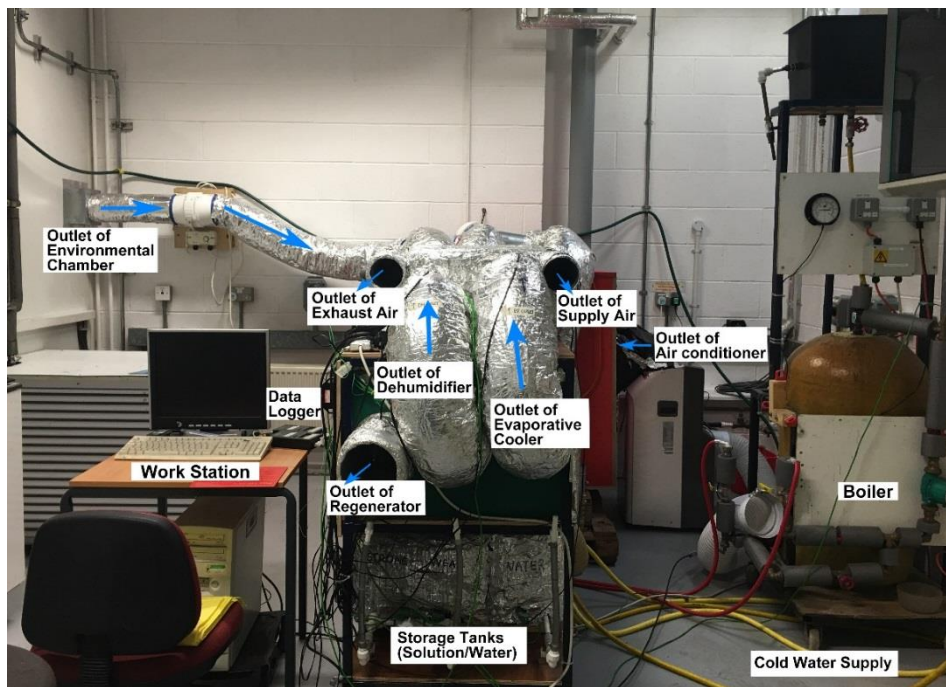
96

Fig. 2. Photo of the membrane-based unit

97

98 **2.1 Experiment method**

99 A boiler is utilized as the heat source for regeneration in the experiment and CaCl₂
 100 solution is selected as the liquid desiccant. A photo of the system test rig is presented
 101 in Fig. 3. Insulations are applied for air ducting, pipe work and heat exchangers to
 102 reduce the surrounding effects. Main experimental equipment with their specifications
 103 is provided in Table 1.



104
 105 Fig. 3. Test rig photo

106 Table 1. Specifications of main equipment

Equipment	Properties		Manufacturer
Magnetic pump	Power	15 W	Shanghai Jiaxing Pumps Co., Ltd.
	Maximum frequency	50 Hz	
	Maximum speed	2600 r/min	
	Maximum capacity	10 L/min	
AC axial fan	Power	45W	ebm-papst Mulfingen
	Nominal speed	2800 min ⁻¹	GmbH & Co. KG
Boiler	Capacity	3kW	Wilo SE
	Supply temperature range	50-80°C	
	Water storage	120 Litre	

	Circulating pump	45W	
	Water flow rate	0-6 L/min	

107 Main measurement instruments with their respective accuracies are listed in Table 2.
108 Series of K-type thermocouples are employed to measure temperatures of desiccant
109 solution and water flows. Humidity and temperature probes are installed at all air inlets
110 and outlets, and associated air velocities are measured with an anemometer. A
111 hydrometer is used to obtain the solution density. Thus, CaCl₂ solution concentration
112 ratio can be determined with correlation on a basis of solution density and temperature
113 [11]. Moreover, volumetric flow rates of liquid flows (i.e. desiccant solution and water)
114 are measured by float-style flow meters, which are calibrated with water at 20°C. In
115 order to equate an actual desiccant solution flow rate in dehumidifier and regenerator
116 units with a reading from the flow meter, the correction correlation given in literature
117 [12] is needed:

$$v_{\text{sol}} = v_{\text{w}} \sqrt{(m_{\text{fl}} - V_{\text{fl}} \rho_{\text{sol}}) \rho_{\text{w}} / (m_{\text{fl}} - V_{\text{fl}} \rho_{\text{w}}) \rho_{\text{sol}}} \quad (1)$$

118 where, v_{sol} and v_{w} are volumetric flow rates of the desiccant solution and water
119 respectively, L/min. ρ_{sol} and ρ_{w} are densities of solution and water, kg/m³. For the
120 flow meter, the float weight (m_{fl}) is 2.1×10^{-3} kg and volume (V_{fl}) is 0.25×10^{-6} m³.

121 Table 2. Specifications of measurement instruments

Devices	Measurement Range	Accuracy
RS K-type thermocouple probe	0-1100°C	±0.75%
Sensirion EK-H4 humidity sensor	-40 - +125°C	±0.3%
	0 - 100% RH	±2%
Parker liquid flow indicator	4-22 L/min	±2%
Testo thermo-anemometer 405	0-10 m/s	±5%
Brannan hydrometer 200 Series	1.0-1.6 g/m ³	±2%
Data logger DT500	Data Acquisition	±0.15%

122

123 The experimental data are processed with uncertainty analysis, which provides the
124 associated error of a calculated value. Error bars are included in the graphs for
125 experimental result analyses.

$$U_y = \sqrt{\sum_{i=1}^N \left(\frac{\partial y}{\partial x_i}\right)^2 \cdot U_{x_i}^2} \quad (2)$$

126 where, U_{x_i} is uncertainty of each measured variable x_i .

127 **2.2 Evaluation Method**

128 *Dehumidification process*

129 The dehumidification performance is assessed by moisture removal rate.

$$\dot{M}_r = \dot{m}_{\text{air_DH}} \cdot (\omega_{\text{in_DH}} - \omega_{\text{out_DH}}) \quad (3)$$

130 where, \dot{M}_r represents moisture removal rate, g/s. $\dot{m}_{\text{air_DH}}$ is mass flow rate of air passing
131 through the dehumidifier, kg/s, $\omega_{\text{in_DH}}$ and $\omega_{\text{out_DH}}$ are air humidity ratios at inlet and
132 outlet of the dehumidifier, kg/kg_{dryair}. Thermophysical properties of the moist air are
133 determined using equations referred to literature [13].

134 The dehumidification effectiveness is defined as the ratio of actual change in moisture
135 content to the maximum moisture transfer.

$$\eta_{\text{DH}} = \frac{\omega_{\text{in_DH}} - \omega_{\text{out_DH}}}{\omega_{\text{in_DH}} - \omega_{\text{eq_DH}}} \quad (4)$$

136 where, η_{DH} is the dehumidification effectiveness. $\omega_{\text{eq_DH}}$ is equilibrium humidity ratio
137 of desiccant solution at the inlet condition, kg/kg_{dryair}. Under the equilibrium state, it is
138 given by literature [14]:

$$\omega_{\text{eq_DH}} = 0.62198 \times \frac{P_{\text{sol}}}{P_{\text{A}} - P_{\text{sol}}} \quad (5)$$

139 where, P_A is atmospheric pressure, Pa, and P_{sol} is vapour pressure of CaCl_2 solution at
140 a given temperature, Pa, which can be calculated with the empirical correlation derived
141 by literature [15].

142 Based on the enthalpy difference between the inlet and outlet air in the dehumidifier,
143 the dehumidifier cooling output is determined as:

$$\dot{Q}_{\text{DH}_c} = \dot{m}_{\text{air_DH}} (h_{\text{in_DH}} - h_{\text{out_DH}}) \quad (6)$$

144 where, \dot{Q}_{DH_c} is the dehumidifier cooling output, W. $h_{\text{in_DH}}$ and $h_{\text{out_DH}}$ are specific
145 enthalpies of air at inlet and outlet of the dehumidifier, J/kg.

146 *Regeneration process*

147 The regeneration performance is evaluated by moisture addition rate.

$$\dot{M}_a = \dot{m}_{\text{air_RE}} \cdot (\omega_{\text{out_RE}} - \omega_{\text{in_RE}}) \quad (7)$$

148 where, \dot{M}_a represents moisture addition rate, g/s. $\dot{m}_{\text{air_RE}}$ is regenerator air mass flow
149 rate, kg/s. $\omega_{\text{in_RE}}$ and $\omega_{\text{out_RE}}$ are humidity ratios of air entering and leaving the
150 regenerator, kg/kg_{dryair}.

151 The thermal input power of the regenerator is determined as:

$$\dot{Q}_{\text{RE}} = \dot{m}_{\text{w_RE}} \cdot c_{\text{p_w_RE}} (T_{\text{w_in}} - T_{\text{w_out}}) \quad (8)$$

152 where, \dot{Q}_{RE} is the regenerator thermal input power, W. $\dot{m}_{\text{w_RE}}$ and $c_{\text{p_w_RE}}$ are water mass
153 flow rate, kg/s, and specific heat capacity, J/kg, in the heating circuit. $T_{\text{w_in}}$ and $T_{\text{w_out}}$
154 are hot water supply and return temperatures respectively, °C.

155 *Coefficient of performance*

156 The total cooling output power of the hybrid system is expressed as:

$$\dot{Q}_c = \dot{m}_{\text{air_DH}} (h_{\text{in_DH}} - h_{\text{supply}}) \quad (9)$$

157 where, \dot{Q}_c is the system total cooling output power, W. h_{supply} is specific enthalpy of
 158 supply air, J/kg.

159 The hybrid system overall coefficients of performance (COP) are defined as:

$$\text{COP}_{\text{th}} = \frac{\dot{Q}_c}{\dot{Q}_{\text{RE}}} \quad (10)$$

$$\text{COP}_{\text{el}} = \frac{\dot{Q}_c}{W_e} \quad (11)$$

160 where, COP_{th} is thermal coefficient of performance and COP_{el} is electrical coefficient
 161 of performance. W_e is electrical consumption, W.

162 3. Results and Discussion

163 Table 3 presents operating variables for the experiment. Effects of operating variables
 164 on the dehumidifier and regenerator performances are investigated at CaCl₂ solution
 165 concentration ratio of 39%.

166 Table 3. Operating variables for experiment

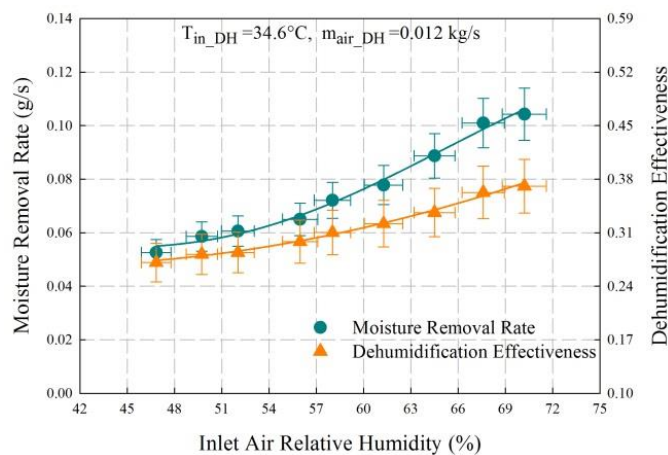
Variables	Range	
<i>Dehumidifier</i>		
Desiccant solution flow rate	1 L/min	
Solution concentration ratio	30-42%	
Air volumetric flow rate	35 m ³ /hr	
Inlet air condition	34-35°C	50-75% RH
<i>Regenerator</i>		
Hot water supply temperature	55-80°C	
Hot water supply flow rate	2 L/min	
Desiccant solution flow rate	1 L/min	
Air volumetric flow rate	44-148 m ³ /hr	
Inlet air condition	26°C	33% RH

<i>Evaporative cooler</i>		
Inlet air condition	26°C	33% RH
Cold water supply temperature	10°C	
Cold water supply flow rate	12 L/min	

167 **3.1 Effect of inlet air relative humidity on dehumidification performance**

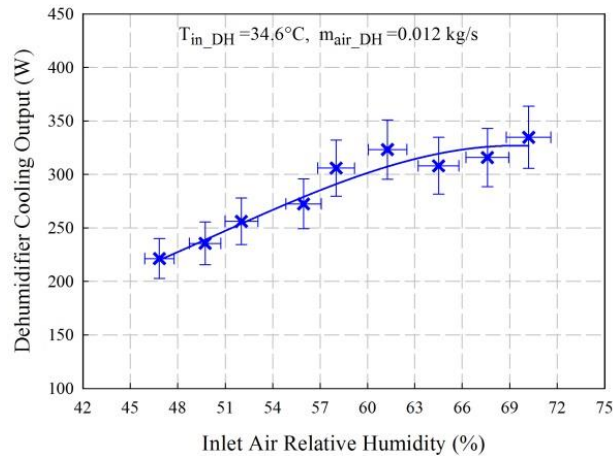
168 The inlet air temperature for the dehumidifier is set at 34.6°C and relative humidity
169 varies from 46% to 70%. It can be seen from Fig. 4(a) that the dehumidifier
170 performance increases with the inlet air relative humidity at the constant inlet air
171 temperature. The dehumidifier moisture removal rate doubles as air relative humidity
172 increases from 46% to 70% and the dehumidification effectiveness improves by 36.9%.
173 The increase in the moisture removal rate is caused by the greater vapour pressure
174 difference between the airstream and desiccant solution.

175 Over the investigated inlet air relative humidity range, the higher inlet air relative
176 humidity leads to more cooling output as shown in Fig. 4(b). The dehumidifier cooling
177 output increases from 221.4W to 334.7W as air relative humidity increases from 46%
178 to 70%. However, as the relative humidity gets higher than 63%, the increase in the
179 cooling output becomes smaller. It indicates that the dehumidifier cooling output
180 approaches the maximum capacity with further increase in air relative humidity.



181
182

(a)



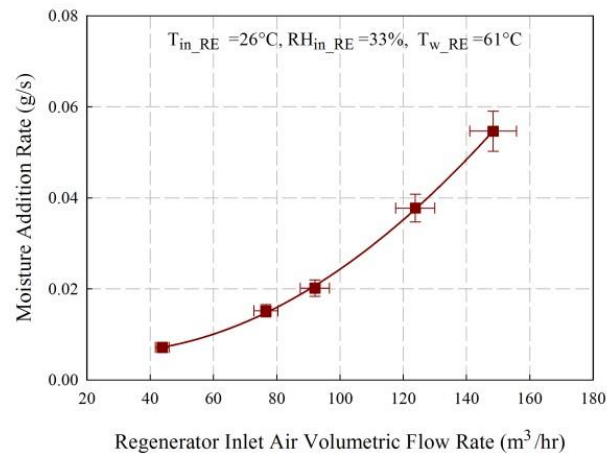
(b)

Fig. 4. Effects of inlet air relative humidity on (a) moisture removal rate and dehumidification effectiveness and (b) dehumidifier cooling output

3.2 Effect of air flow rate on regeneration performance

Tests are carried out to investigate air flow rate effect on the regeneration performance.

At an inlet air temperature of 26°C and relative humidity of 33%, the regenerator air flow rate is increased from 43.82m³/hr to 148.44m³/hr, while the hot water is kept at a temperature of 61°C. Though the increase of regenerator air flow rate leads to reduction in the moisture addition capability, the moisture addition rate takes both the moisture content change and air flow rate into account. As observed in Fig. 5, there is an increase in the moisture addition rate. However, the moisture addition rate only increases by 0.04g/s over the investigated air flow rate range, which indicates that the impact of the air flow rate on regeneration performance is not very significant.

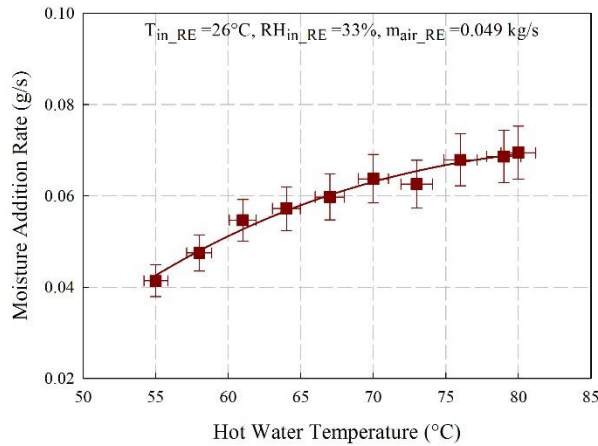


197
198

Fig. 5. Effects of air flow rate on moisture addition rate

199 3.3 Effect of hot water temperature on regeneration performance

200 To identify the effect of hot water temperature on regeneration performance, the hot
 201 water is supplied in the temperature range from 55°C to 80°C. As presented in Fig. 6,
 202 the regeneration performance improves accordingly with hot water temperature under
 203 the constant regenerator inlet condition. The moisture addition rate increases by 75%
 204 as the hot water temperature increases from 55°C to 80°C. The increase in hot water
 205 temperature results in higher desiccant solution temperature in the regenerator, and thus
 206 higher vapour pressure is obtained in solution side. Then the greater vapour pressure
 207 difference between the desiccant solution and airstream leads to more mass transfer in
 208 the regeneration process at the constant inlet air condition. Moreover, as the hot water
 209 temperature is above 70°C, it is noted that the increase in the moisture addition rate
 210 becomes smaller. The variation in the air humidity ratio across the regenerator is only
 211 0.06g/kg_{dryair} as the hot water temperature rises from 70°C to 80°C. Therefore,
 212 regarding to the feasibility of utilizing renewable energy as heat source, at the given
 213 operating condition, hot water supply temperature up to 70°C is sufficient for adequate
 214 regeneration performance.

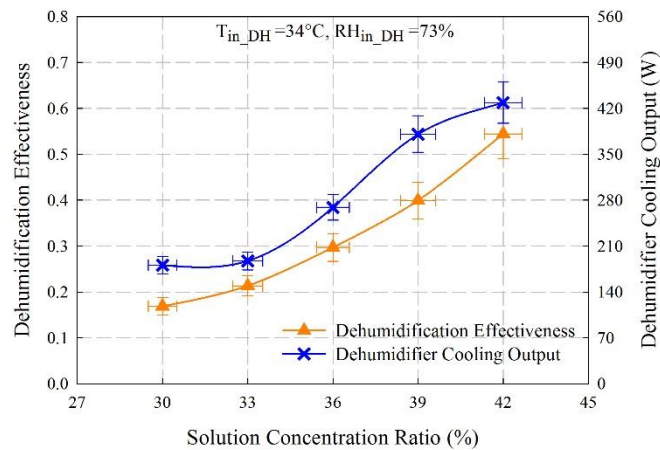


215
216

Fig. 6. Effect of hot water temperature on moisture addition rate

217 3.4 Effect of concentration ratio on system performance

218 According to the operative concentration ratio level of CaCl_2 , investigations are
 219 conducted with solution concentration ratio ranging from 30% to 42%. The
 220 dehumidification effectiveness increases evidently with concentration ratio as shown in
 221 Fig. 7. For desiccant solution concentration ratio below 33%, there is only slight
 222 difference in the dehumidifier effectiveness, which implies the operative concentration
 223 ratio needs to be at least above 33%. As solution concentration ratio gets higher than
 224 33%, the dehumidifier effectiveness improves more significantly and reaches up to 0.54
 225 at concentration ratio of 42%. For operation of the liquid desiccant system, higher
 226 desiccant solution concentration ratio would be better for dehumidification
 227 performance. However, the use of highly concentrated solution may cause salt
 228 crystallization, which may lead to risks of fluid mal-distribution, channel blockage,
 229 high pumping pressure, and membrane fouling. On the other hand, the dehumidifier
 230 cooling output also increases from 181.0W to 428.8W with the increase of solution
 231 concentration ratio, which is related to the higher moisture removal rate in the
 232 dehumidifier.



233

234

Fig. 7. Effects of solution concentration ratio on dehumidification effectiveness and cooling output

235

It can be observed from Fig. 8 that as concentration ratio increases from 30% to 42%,

236

the dehumidifier moisture removal rate improves from 0.05g/s to 0.14g/s while the

237

regenerator moisture addition rate decreases from 0.11g/s to 0.05g/s. For the

238

dehumidification process, the driving force caused by the vapour pressure difference

239

between airstream and desiccant solution gets higher for stronger solution, which thus

240

leads to greater moisture removal rate in the dehumidifier. On the contrary, in the

241

regeneration process, desiccant solution with higher concentration ratio has lower

242

capability for moisture addition due to the lower vapour pressure.

243

To allow continuous operation of the overall system, the performance of regenerator

244

should match with that of dehumidifier otherwise mass imbalance occurs, which would

245

result in some problems such as the dilution of desiccant solution over time. For the

246

investigated operating condition, the dehumidification and regeneration processes are

247

balanced at desiccant solution concentration ratio of 36%, as the dehumidifier moisture

248

removal rate equals to the regenerator moisture addition rate. Thus, measures are

249

needed to facilitate the regenerator performance for the stronger desiccant solution

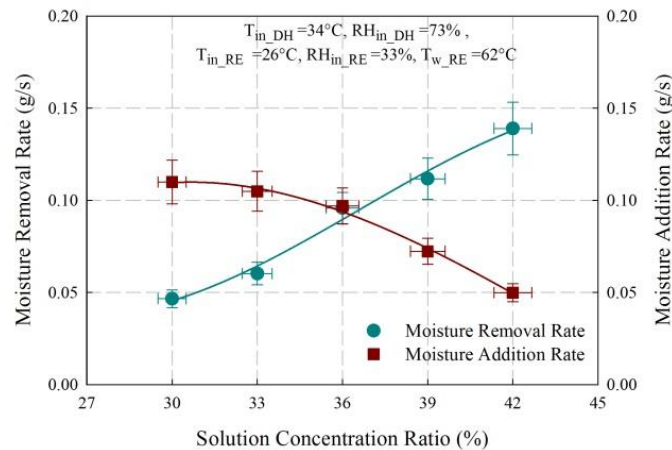
250

while the dehumidification performance should be improved at lower concentration

251

ratio. Under the system steady operation condition, the thermal COP_{th} and electrical

252 COP_{el} reach up to 0.70 and 2.62 respectively at concentration ratio of 36%, while the
 253 supply air temperature is provided at 20.4°C. Hence, the results reveal that the hybrid
 254 system is feasible for applications, and the supply air condition could meet the
 255 comfortable indoor environment requirement.



256
 257

Fig. 8. Effects of solution concentration ratio on moisture removal and addition rates

258 4. Conclusions

259 A membrane-based hybrid liquid desiccant dehumidification cooling system is
 260 developed to provide efficient temperature and humidity controls in hot and humid
 261 regions. The experimental results indicate the system with CaCl₂ desiccant solution is
 262 feasible for dehumidification and cooling purposes under the tested hot and humid
 263 conditions. Impacts of operating variables on dehumidifier, regenerator and system
 264 performances are identified through experimental tests. As inlet air relative humidity
 265 increases from 46% to 70% at constant temperature of 34.6°C, the dehumidifier
 266 moisture removal rate doubles and dehumidification effectiveness improves by 36.9%.
 267 On the other hand, the regenerator performance increases with inlet air flow rate and
 268 hot water temperature. As the hot water temperature increases from 55°C to 80°C, the
 269 regenerator moisture addition rate increases by 75% under the same inlet air condition.
 270 By increasing the desiccant solution concentration ratio from 30% to 42%, the

271 dehumidification performance improves from 0.05g/s to 0.14g/s and the dehumidifier
272 cooling output doubles, while the regenerator moisture addition rate decreases by
273 54.5%. For steady system operation, mass balance between dehumidification and
274 regeneration is of vital importance. Under the investigated solution concentration ratio
275 of 36%, the supply air temperature of 20.4°C is obtained, the system thermal COP_{th}
276 achieves up to 0.70 and electrical COP_{el} reaches to 2.62 accordingly.

277 **Acknowledgements**

278 The authors gratefully acknowledge the scholarship support from the Faculty of
279 Engineering of the University of Nottingham.

280 **References**

- 281 [1] K. Daou, R. Wang, and Z. Xia, "Desiccant cooling air conditioning: a review,"
282 *Renewable and Sustainable Energy Reviews*, vol. 10, pp. 55-77, 2006.
- 283 [2] X. Wang, W. Cai, J. Lu, Y. Sun, and X. Ding, "Heat and Mass Transfer Model
284 for Desiccant Solution Regeneration Process in Liquid Desiccant
285 Dehumidification System," *Industrial & Engineering Chemistry Research*, vol.
286 53, pp. 2820-2829, 2014.
- 287 [3] L.-Z. Zhang, "Progress on heat and moisture recovery with membranes: From
288 fundamentals to engineering applications," *Energy Conversion and
289 Management*, vol. 63, pp. 173-195, 2012.
- 290 [4] S. Y. Ahmed, P. Gandhidasan, and A. A. Al-Farayedhi, "Thermodynamic
291 analysis of liquid desiccants," *Solar Energy*, vol. 62, pp. 11-18, 1998.
- 292 [5] L. Mei and Y. J. Dai, "A technical review on use of liquid-desiccant
293 dehumidification for air-conditioning application," *Renewable and Sustainable
294 Energy Reviews*, vol. 12, pp. 662-689, 2008.

- 295 [6] R. Qi, L. Lu, and Y. Jiang, "Investigation on the liquid contact angle and its
296 influence for liquid desiccant dehumidification system," *International Journal*
297 *of Heat and Mass Transfer*, vol. 88, pp. 210-217, 2015.
- 298 [7] S.-M. Huang and L.-Z. Zhang, "Researches and trends in membrane-based
299 liquid desiccant air dehumidification," *Renewable and Sustainable Energy*
300 *Reviews*, vol. 28, pp. 425-440, 2013.
- 301 [8] A. H. Abdel-Salam, G. Ge, and C. J. Simonson, "Thermo-economic
302 performance of a solar membrane liquid desiccant air conditioning system,"
303 *Solar Energy*, vol. 102, pp. 56-73, 4// 2014.
- 304 [9] H. T. El-Dessouky, H. M. Ettouney, and W. Bouhamra, "A Novel Air
305 Conditioning System," *Chemical Engineering Research and Design*, vol. 78, pp.
306 999-1009, 2000.
- 307 [10] M. Jradi and S. Riffat, "Experimental investigation of a biomass-fuelled micro-
308 scale tri-generation system with an organic Rankine cycle and liquid desiccant
309 cooling unit," *Energy*, vol. 71, pp. 80-93, 2014.
- 310 [11] Å. Melinder, *Thermophysical Properties of Aqueous Solutions Used as*
311 *Secondary Working Fluids [Elektronisk resurs]*. Stockholm: KTH, 2007.
- 312 [12] S. Liu, "A novel heat recovery/desiccant cooling system," PhD, Architecture
313 and Built Environment, University of Nottingham, 2008.
- 314 [13] P. T. Tsilingiris, "Thermophysical and transport properties of humid air at
315 temperature range between 0 and 100 °C," *Energy Conversion and Management*,
316 vol. 49, pp. 1098-1110, 5// 2008.
- 317 [14] ASHRAE, "2013 ASHRAE Handbook - Fundamentals (I-P Edition)," ed:
318 American Society of Heating, Refrigerating and Air-Conditioning Engineers,
319 Inc., 2013.

320 [15] L. A. Cisternas and E. J. Lam, "An analytic correlation for the vapour pressure
321 of aqueous and non-aqueous solutions of single and mixed electrolytes. Part II.
322 Application and extension," *Fluid Phase Equilibria*, vol. 62, pp. 11-27, 1991.

323